

Durham Research Online

Deposited in DRO:

27 May 2016

Version of attached file:

Accepted Version

Peer-review status of attached file:

Peer-reviewed

Citation for published item:

Pogge von Strandmann, P.A.E. and Burton, K.W. and Opfergelt, S. and Eiríksdóttir, E.S. and Murphy, M.J. and Einarsson, A. and Gíslason, S.R. (2016) 'The effect of hydrothermal spring weathering processes and primary productivity on lithium isotopes : Lake Myvatn, Iceland.', *Chemical geology.*, 445 . pp. 4-13.

Further information on publisher's website:

<http://dx.doi.org/10.1016/j.chemgeo.2016.02.026>

Publisher's copyright statement:

© 2016 This manuscript version is made available under the CC-BY-NC-ND 4.0 license
<http://creativecommons.org/licenses/by-nc-nd/4.0/>

Additional information:

Use policy

The full-text may be used and/or reproduced, and given to third parties in any format or medium, without prior permission or charge, for personal research or study, educational, or not-for-profit purposes provided that:

- a full bibliographic reference is made to the original source
- a [link](#) is made to the metadata record in DRO
- the full-text is not changed in any way

The full-text must not be sold in any format or medium without the formal permission of the copyright holders.

Please consult the [full DRO policy](#) for further details.

1 **The effect of hydrothermal spring weathering processes and primary**
2 **productivity on lithium isotopes: Lake Myvatn, Iceland**

3

4 Philip A.E. Pogge von Strandmann¹, Kevin W. Burton², Sophie Opfergelt³, Eydís S.
5 Eiríksdóttir⁴, Melissa J. Murphy⁵, Arni Einarsson^{6,7}, Sigurdur R. Gislason⁴

6

7 ¹Institute of Earth and Planetary Sciences, University College London and
8 Birkbeck, University of London, Gower Street, London, WC1E 6BT, UK.

9 ²Department of Earth Sciences, Durham University, Durham, DH1 3LE, UK.

10 ³Earth and Life Institute, Université catholique de Louvain, Croix du Sud 2 bte
11 L7.05.10, 1348 Louvain-la-Neuve, Belgium.

12 ⁴Institute of Earth Sciences, University of Iceland, Reykjavik, Iceland.

13 ⁵Department of Earth Sciences, Oxford University, South Parks Road, Oxford, UK.

14 ⁶Myvatn Research Station, Skútutstadir, Myvatn, Iceland.

15 ⁷Institute of Life- and Environmental Sciences, University of Iceland, Reykjavik,
16 Iceland

17

18 Lithium isotopes are rapidly becoming one of the most useful tracers of silicate
19 weathering processes, but little is known on their behaviour in groundwaters
20 and hydrothermal springs, and how these sources might influence the
21 weathering signal in surface waters. This study presents lithium isotope
22 compositions ($\delta^7\text{Li}$) for cold groundwaters (3–7°C) and hydrothermal springs
23 that were at geothermal temperatures (200–300°C) but have cooled during
24 transport (17–44°C). Both represent an important source of water and nutrients
25 for Lake Myvatn, Iceland. We also present a time-series from the Laxa River,
26 which is the single outflow from the lake. The $\delta^7\text{Li}$ values in the input springs to
27 Lake Myvatn are highly variable (5–27‰), and correlate inversely with
28 temperature and total dissolved solids. These co-variations imply that even in
29 such waters, the processes controlling $\delta^7\text{Li}$ variations during weathering still
30 operate: that is, the ratio of primary rock dissolution to secondary mineral
31 formation, where the latter preferentially incorporates ^6Li with a temperature-
32 dependent fractionation factor. In high-temperature geothermal waters
33 (>300°C) secondary mineral formation is inhibited, and has a low fractionation

34 factor, leading to little $\delta^7\text{Li}$ fractionation. Even in waters that have cooled
35 considerably over several months from their geothermal temperatures,
36 fractionation is still low, and $\delta^7\text{Li}$ values are similar to those reported from
37 waters measured at $>350^\circ\text{C}$. In contrast, cooler groundwaters promote relatively
38 high proportions of clay formation, which scavenge dissolved solids (including
39 ^6Li). The time series on the Laxa River, the single outflow from Lake Myvatn,
40 shows little $\delta^7\text{Li}$ variation with time over the 12 month sampling period (17-
41 21‰), demonstrating that in contrast to tracers such as Si isotopes, Li isotopes
42 are unaffected by the significant seasonal phytoplankton blooms that occur in
43 the lake. Thus, these results clearly illustrate that Li isotopes are ideally suited to
44 constrain silicate weathering processes, because fractionation by secondary
45 mineral formation operates even when groundwater and hydrothermal inputs
46 are significant, and because Li isotopes are demonstrably unaffected by
47 phytoplankton or plant growth.

48

49 1.0 Introduction

50 The chemical weathering of continental Ca-Mg silicates is one of the primary
51 processes that remove atmospheric CO_2 , causing it to eventually be sequestered
52 in the oceans and carbonate rocks (Berner, 2003; Walker et al., 1981). Chemical
53 weathering also affects the carbonate saturation state of the oceans on shorter,
54 millennial, timescales, affecting its pH and ability to store CO_2 (Archer et al.,
55 2000). Therefore, silicate weathering is a critical part of the carbon cycle, and is a
56 process that urgently requires accurate quantification, both in the present, and in
57 the past. Without these data, our knowledge regarding the mechanisms and rates
58 of climate stabilisation is lacking. The weathering of basalts, in particular, exerts
59 a greater effect on global CO_2 budgets than would be anticipated from the extent
60 of global basaltic terrains (Dessert et al., 2003; Gaillardet et al., 1999; Gislason,
61 2005; Gislason et al., 2009), and therefore is a fruitful area to examine global
62 weathering processes.

63 Traditionally, radiogenic isotopes (e.g. $^{87}\text{Sr}/^{86}\text{Sr}$) have been used to
64 understand weathering processes, and quantify palaeo-weathering (Allegre et al.,
65 2010; Blum and Erel, 1997; Jones and Jenkyns, 2001; Raymo et al., 1988).
66 However, such systems tend to be strongly influenced by the isotope ratio of the

67 rock undergoing weathering, and, importantly, often cannot distinguish between
68 weathering of silicates over carbonates (where the latter does not sequester
69 atmospheric CO₂ over geologic time) (Oliver et al., 2003; Palmer and Edmond,
70 1992). Hence, novel isotopic tracers of weathering have been sought that are
71 independent of lithology and other non-weathering processes, such as biology.
72 Lithium isotopes (⁶Li and ⁷Li, where the ratio is reported as δ⁷Li) have proved to
73 be one of the most useful of these tracers, and are currently the only known
74 tracer that solely responds to silicate weathering processes (Pogge von
75 Strandmann and Henderson, 2015). This is because the Li isotope ratio is
76 thought to be unaffected by uptake into plants (Lemarchand et al., 2010), and
77 because Li, even in carbonate catchments, is demonstrably dominantly sourced
78 from silicates (Kisakürek et al., 2005; Millot et al., 2010b). The Li isotope ratio of
79 silicate rocks describes a very narrow range (δ⁷Li_{continental crust} ~ 0.6 ± 0.6‰
80 (Sauzeat et al., 2015; Teng et al., 2004); δ⁷Li_{basalt} = ~3–5‰ (Elliott et al., 2006;
81 Tomascak et al., 2008)), relative to that reported in river waters (δ⁷Li = 2–44‰;
82 global mean 23‰ (Dellinger et al., 2015; Huh et al., 2001; Huh et al., 1998;
83 Kisakürek et al., 2005; Lemarchand et al., 2010; Liu et al., 2015; Millot et al.,
84 2010b; Pogge von Strandmann et al., 2010; Pogge von Strandmann et al., 2006;
85 Pogge von Strandmann and Henderson, 2015; Pogge von Strandmann et al.,
86 2012; Pogge von Strandmann et al., 2014b; Rad et al., 2013; Vigier et al., 2009;
87 Wang et al., 2015; Wimpenny et al., 2010b; Witherow et al., 2010)). This high
88 variability in rivers is caused by weathering processes: dissolution of silicates
89 causes no isotope fractionation, but secondary minerals formed during
90 weathering preferentially take up ⁶Li, driving residual waters isotopically heavy
91 (Huh et al., 2001; Pistiner and Henderson, 2003; Pogge von Strandmann et al.,
92 2010; Vigier et al., 2008; Wimpenny et al., 2010a). Therefore, surface water δ⁷Li
93 is controlled by the ratio of primary mineral dissolution (low δ⁷Li, high [Li])
94 relative to secondary mineral formation (driving waters to high δ⁷Li, and low
95 [Li]). This ratio has also been described as the weathering congruency (Misra
96 and Froelich, 2012; Pogge von Strandmann et al., 2013), weathering efficiency
97 (Pogge von Strandmann and Henderson, 2015) or weathering intensity
98 (Dellinger et al., 2015): when riverine δ⁷Li = rock δ⁷Li, then weathering is
99 congruent (water chemistry = rock chemistry), efficient (cations are not retained

100 in clays, but are delivered to the oceans) and low intensity (little clay formation,
101 and a low weathering to denudation ratio – bearing in mind that “weathering
102 intensity” has been used in different ways by different authors).

103 A considerable body of literature has built up over the past decades on
104 riverine Li behaviour (Bagard et al., 2015; Dellinger et al., 2014; Huh et al., 2001;
105 Huh et al., 1998; Kusakürek et al., 2005; Lemarchand et al., 2010; Liu et al., 2015;
106 Millot et al., 2010b; Pistiner and Henderson, 2003; Pogge von Strandmann et al.,
107 2010; Pogge von Strandmann et al., 2006; Pogge von Strandmann and
108 Henderson, 2015; Pogge von Strandmann et al., 2008b; Pogge von Strandmann et
109 al., 2012; Pogge von Strandmann et al., 2014b; Rad et al., 2013; Teng et al., 2010;
110 Vigier et al., 2009; Wang et al., 2015; Wimpenny et al., 2010b; Witherow et al.,
111 2010), and more recently, forays into palaeo-weathering have emerged (Hall et
112 al., 2005; Hathorne and James, 2006; Hoefs and Sywall, 1997; Lechler et al., 2015;
113 Misra and Froelich, 2012; Pogge von Strandmann et al., 2013; Ullmann et al.,
114 2013). However, groundwaters, and their influence on weathering and the
115 continental Li isotope signal, remain poorly characterised (Bagard et al., 2015;
116 Hogan and Blum, 2003; Meredith et al., 2013; Negrel et al., 2010; Negrel et al.,
117 2012; Pogge von Strandmann et al., 2014b; Tomascak et al., 2003), as does the
118 potential influence of land-based hydrothermal groundwaters and springs
119 (Henchiri et al., 2014; Millot et al., 2010a; Pogge von Strandmann et al., 2010;
120 Pogge von Strandmann et al., 2006). It is clear, however, that continental
121 hydrothermal systems (including island arcs and ocean islands) can have very
122 high Li concentrations (up to ~37 mmol/l (Chan et al., 1993; Chan et al., 1994;
123 Millot et al., 2010a)), and therefore may influence the global riverine isotope
124 composition, given the high significance of basaltic weathering to the global
125 mean (Dessert et al., 2003; Gaillardet et al., 1999). Changes in this input over
126 time may also have led to changes in the global mean riverine and groundwater
127 composition, and therefore groundwater and riverine fluxes to the oceans, as has
128 also been proposed for the Sr isotope system (Allegre et al., 2010).

129 This study presents Li isotope data for hydrothermal groundwaters that
130 comprise the dominant source of Lake Myvatn, in northern Iceland. These waters
131 have experienced water-rock interactions at a range of temperatures, from
132 ~300°C (cooled during transport to 17–44°C) hydrothermal springs to cold

133 groundwaters (3–7°C). This approach allows the comparison of “hot” and “cold”
134 groundwaters from the same region, and their individual impact on Li isotope
135 behaviour. Both groundwater types may, in many global regions, have significant
136 impact on river water chemistry. We also report Li isotope data for a time series
137 from the Laxa River, the single outflow from the lake, to constrain how seasonal
138 variations in biological productivity potentially affect Li isotopes. The latter is
139 important, as it provides a natural laboratory to study the effects of significant
140 variation in primary productivity and biocycling on Li isotopes. These data will
141 be compared with previously published silicon isotope data for the same
142 samples which show large variations in both isotope composition and elemental
143 abundances due to seasonal diatom blooms within the lake (Opfergelt et al.,
144 2011). It has been shown that some plants do not fractionate Li isotopes
145 (Lemarchand et al., 2010), but that study remains the only assertion that Li
146 isotopes are not fractionated during biological uptake. It is therefore important
147 to test this assumption, to determine whether Li isotopes are really such a useful
148 tracer of silicate weathering processes in isolation from any biological effects.

149

150 2.0 Field area and samples

151 Lake Myvatn is a shallow eutrophic lake in NE Iceland (65°35'N,
152 17°00'W), located just beneath the Arctic Circle (Fig. 1). The lake is at 278 m
153 above sea level, and has a maximum depth of 4.2 m, and an area of 37 km².
154 During the ice-free season (mid May to late September), the entire water column
155 is well-mixed. The lake is almost entirely groundwater fed, with cold springs
156 feeding the southern basin (Sydrifloi), and warm springs feeding the northern
157 basin (Ytrifloi). The latter springs gain their heat from the Namafjall and Krafla
158 geothermal fields (Kristmannsdottir and Armannsson, 2004). The main outflow
159 from the lake is via the Laxa River, yielding a residence time for water in the lake
160 of about 27 days (Olafsson, 1979) (Fig. 1).

161 The lake was formed ~2300 years ago by a major basaltic volcanic
162 eruption (Hauptfleisch and Einarsson, 2012; Thordarson and Hoskuldsson,
163 2002). This underlying geology has been modified during more recent eruptions,
164 such as the 1725–1729 and 1975–1984 eruptions in the Krafla Volcano, 10km to
165 the north (Thordarson and Hoskuldsson, 2002).

166 The lake is one of the most productive in the northern hemisphere,
167 despite winter ice cover. This is related largely to nutrient-rich groundwater
168 inflow, reflected by very high seasonal diatom, green algae and cyanobacteria
169 productivity (Gislason et al., 2004). The concentrations of many dissolved metals
170 in the lake are largely controlled by biological activity. In the ice-covered winter,
171 the top sediment pore waters are enriched in nutrients by several orders of
172 magnitude relative to the lake waters. These nutrients are released in the ice-
173 free summer by bioturbation, sediment resuspension and diffusion, leading to
174 high nutrient fluxes (Gislason et al., 2004).

175 Samples were taken from both the “cold” and “hot” springs sourcing the
176 lake, and a monthly time series spanning March 2000 to March 2001 was taken
177 from the Laxa River draining the lake following sampling protocols outlined in
178 Opfergelt et al., 2011.

179

180 3.0 Methods

181 Major and trace element concentrations are from Opfergelt et al., 2011,
182 and were determined by ICP-MS and ion chromatography. For Li isotope
183 analysis, 15 ml of sample was dried down, and passed through a two-step cation
184 exchange chromatography (AG50W X-12), using dilute HCl as an eluent. Isotopic
185 analyses were conducted on a Nu Instruments multi-collector ICP-MS, relative to
186 the standard L-SVEC (Flesch et al., 1973). The exact methods for chemistry and
187 analysis are detailed elsewhere (Pogge von Strandmann et al., 2011; Pogge von
188 Strandmann and Henderson, 2015; Pogge von Strandmann et al., 2013).

189 Seawater was run as an “unknown” standard, yielding $\delta^7\text{Li} = 31.3 \pm 0.6\text{‰}$ (n=48,
190 chemistry=48) over a three-year period. The total procedural blank of this
191 method was effectively undetectable (<0.005ng Li), which is insignificant relative
192 to the 10–20 ng of Li analysed in each sample.

193 The groundwater and river elemental concentrations were used to
194 calculate mineral saturation states using PHREEQC (Parkhurst and Appelo,
195 1999). These are reported as SI, the saturation index, which is a logarithmic
196 scale, with positive numbers indicating oversaturation, and negative numbers
197 undersaturation. The uncertainty depends on the individual mineral, but is
198 typically around 1–2 log units (Stefansson and Gislason, 2001).

199

200 4.0 Results

201 *4.1 Mineral saturation*

202 Groundwater pH, generally the dominant control on mineral saturation in
203 Iceland (Gíslason et al., 1996; Stefansson and Gíslason, 2001; Stefansson et al.,
204 2001), varies between 8.1 and 10.0 (Table 1 – groundwater pH was measured at
205 spring temperature, while outflow pH was measured at room temperature
206 (Opfergelt et al., 2011)). Consequently, primary minerals, such as forsterite, are
207 significantly undersaturated (Stefansson et al., 2001). Clay minerals such as
208 kaolinite and smectites are oversaturated between pH 8–9.5, and undersaturated
209 at pH >9.5, as are zeolites (common zeolites like laumontite or phillipsite are at
210 or below saturation at pH >9 in these waters). In contrast, minerals such as
211 chlorite tend to dominate at high pH. This is similar to the trends observed in
212 Icelandic rivers (Gíslason et al., 1996; Pogge von Strandmann et al., 2008a; Pogge
213 von Strandmann et al., 2006; Stefansson and Gíslason, 2001; Stefansson et al.,
214 2001).

215 Mineral saturation in the Laxa time series varies strongly with time.
216 Primary minerals, such as forsterite, are highly undersaturated in the winter, and
217 approach saturation in the summer. In contrast, secondary minerals such as
218 kaolinite and smectite are undersaturated only in the summer. Calcite becomes
219 oversaturated at highest pH during the summer.

220

221 *4.2 Lithium*

222 Lithium concentrations in the groundwater samples vary between 130
223 and 10,000 nmol/l, and between 116 and 237 nmol/l in the Laxa River outflow
224 (Table 1). These concentrations are up to two orders of magnitude higher than
225 those in most Icelandic rivers, although similar to other hydrothermal springs,
226 and rivers affected by them (Louvat et al., 2008; Pogge von Strandmann et al.,
227 2006; Vigier et al., 2009). Equally, the concentrations in Icelandic soil pore
228 waters are also generally similar to these springs (Pogge von Strandmann et al.,
229 2012).

230 Lithium isotope ratios ($\delta^7\text{Li}$) vary between 5.1 and 27.2‰ in the springs,
231 showing a negative correlation with Li concentration (shown as the reciprocal in

232 Fig. 2), as well as with temperature, and total dissolved solids concentration.
233 Similar correlations with concentration have been observed in many rivers,
234 groundwaters and pore waters, reflecting the controlling factors on Li, namely
235 primary mineral dissolution to secondary mineral formation (Kisakürek et al.,
236 2005; Millot et al., 2010b; Pogge von Strandmann et al., 2010; Pogge von
237 Strandmann et al., 2006; Pogge von Strandmann and Henderson, 2015; Pogge
238 von Strandmann et al., 2012; Pogge von Strandmann et al., 2014b). Relatively
239 low $\delta^7\text{Li}$ (1–11‰) have been observed in other high-temperature hydrothermal
240 springs, both from Iceland (Pogge von Strandmann et al., 2006), and other
241 basaltic terrains (Millot et al., 2010a; Pogge von Strandmann et al., 2010).
242 Equally, the global mean hydrothermal input to the oceans at mid-ocean ridges is
243 thought to be $\sim 8\%$ (Chan et al., 1993; Chan et al., 1994; Hathorne and James,
244 2006; Misra and Froelich, 2012).

245 In contrast, $\delta^7\text{Li}$ in the Laxa varies much less (17.2–20.8‰), with no
246 obvious time-dependent trends. This is a narrow range, compared to other
247 Icelandic rivers (15–44‰), where values of $\sim 10\%$ have been reported in rivers
248 with high hydrothermal influence (Pogge von Strandmann et al., 2006; Vigier et
249 al., 2009).

250

251 5.0 Discussion

252 *5.1 Hydrothermal springs*

253 As with most aqueous systems, and particularly relatively simple systems
254 sourced solely by basalt (Liu et al., 2015; Pogge von Strandmann et al., 2010;
255 Pogge von Strandmann et al., 2006; Pogge von Strandmann et al., 2012), the
256 springs sourcing Myvatn exhibit a negative co-variation between $\delta^7\text{Li}$ and Li
257 concentrations (Fig. 2). This co-variation confirms that Li isotopes in these
258 springs are being controlled by the same processes that dominate Li isotopes in
259 other weathering environments, namely the ratio of primary mineral dissolution
260 to secondary mineral formation. Because secondary minerals preferentially take
261 up ^6Li , when their formation rate is relatively high, they will deplete waters in Li,
262 and drive them to higher $\delta^7\text{Li}$. This process has been observed in most global
263 river catchments, and also likely operates for the global mean riverine flux to the
264 oceans. At hydrothermal temperatures, however, different secondary minerals

265 form compared to low temperature environments. At up to $\sim 200^{\circ}\text{C}$, smectites,
266 zeolites and mixed-layer clays dominate, while chlorites dominate at 250°C , and
267 by $\sim 300^{\circ}\text{C}$ secondary minerals that fractionate Li do not form at all, and
268 alteration minerals such as epidote or actinolite are common (Henley and Ellis,
269 1983). At the same time, higher temperatures result in lower isotopic
270 fractionation factors, and experimental evidence suggests that smectite causes
271 $<2\text{‰}$ fractionation at 250°C (Vigier et al., 2008). Analyses of altered basalt
272 suggests that at these temperatures, chlorite causes similar fractionation
273 (Verney-Carron et al., 2015). Experiments and data that approach Li isotope
274 fractionation from the high-temperature end, however, suggest that fluids should
275 be around 6.5‰ higher than corresponding solids at 250°C , and 5.5‰ higher at
276 300°C (Chan et al., 1993; Marschall et al., 2007; Wunder et al., 2006). Hence,
277 there is some ambiguity on the exact fractionation caused by secondary minerals
278 at these temperatures, and hence whether a lack of fractionation is caused by a
279 low fractionation factor, and/or whether fractionating minerals are sparsely
280 present.

281 The $\delta^7\text{Li}$ of the springs co-varies negatively with both temperature (3–
282 44°C) and conductivity. The $\delta^7\text{Li}$ values of the higher temperature waters (~ 5 –
283 10‰) are similar those reported from significantly hotter hydrothermal waters,
284 both at mid-ocean ridges (6 – 11‰ , temp = 270 – 350°C (Chan et al., 1993; Chan et
285 al., 1994)), and in continental volcanic settings (1.0 – 10.9‰ , temp = 33 – 250°C)
286 (Millot et al., 2010a; Pogge von Strandmann et al., 2010; Pogge von Strandmann
287 et al., 2006; Pogge von Strandmann and Henderson, 2015). In a series of
288 hydrothermal experiments, both Chan et al. (1994) and Millot et al. (2010a)
289 showed that the $\delta^7\text{Li}$ of hydrothermal fluids decreases with higher temperatures.
290 The $\delta^7\text{Li}$ of the fluids reached $\sim 5\text{‰}$ (basaltic values) at $\sim 350^{\circ}\text{C}$, due to more
291 efficient leaching of basalt at higher temperatures promoting isotopic
292 equilibration with the host rock, and particularly, a lack of secondary mineral
293 formation at higher temperatures (Henley and Ellis, 1983) and lower isotopic
294 fractionation factors in those minerals that still form at those temperatures. In
295 the Myvatn spring samples, a similar trend is observed, but values of $\sim 5\text{‰}$ are
296 achieved at temperatures $\sim 20^{\circ}\text{C}$. This suggests that the “hot” Myvatn springs
297 were at significantly higher temperatures in the Krafla geothermal fields, and

298 cooled during their at least two month's travel (Kristmannsdottir and
299 Armannsson, 2004) to Myvatn, preserving their original isotopic signature.
300 Hence, despite the 200–250°C cooling the “hot” springs have undergone
301 (Bodvarsson et al., 1984), relatively little effect by secondary mineral formation
302 has occurred, causing a maximum $\delta^7\text{Li}$ fractionation of around 6‰ from basalt.

303 In contrast, the “cold” groundwater springs are highly fractionated from
304 basalt, with $\delta^7\text{Li}$ values up to 27‰ (23‰ higher than basalt), likely due to the
305 formation of secondary minerals such as smectites or zeolites. This therefore
306 agrees with the hypothesis of Millot et al., (2010a), that temperature is a direct
307 control on hydrothermal fluid $\delta^7\text{Li}$, via inhibition of secondary mineral formation
308 and depression of fractionation factors.

309 Overall, several different reaction-flow models (Bouchez et al., 2013; Liu
310 et al., 2015; Pogge von Strandmann et al., 2014b; Wanner et al., 2014) have
311 proposed that it is the water-rock interaction time that controls riverine Li
312 isotope ratios. For rivers with significant hydrothermal input, this effect may be
313 diluted, because of the input of waters that have had high water-rock interaction
314 time at high temperatures will still have unfractionated Li isotope ratios. Hence,
315 Li isotopes will likely not function as a tracer of water-rock interaction in rivers
316 with a hydrothermal input.

317

318 5.1.1 Elemental mobility and weathering tracers

319 Warmer spring waters generally have more Na, K, Ca and Si than the
320 colder waters, as well as low $\delta^7\text{Li}$ values (see above). Low dissolved $\delta^7\text{Li}$ values
321 suggest a high ratio of primary rock dissolution relative to secondary mineral
322 formation. In other words, the lower and more rock-like the dissolved $\delta^7\text{Li}$ is, the
323 more nominally congruent silicate weathering is (relatively less secondary
324 mineral formation). As discussed above, it is also possible that rock-like $\delta^7\text{Li}$
325 values are due to a lack of isotope fractionation at higher temperatures (Verney-
326 Carron et al., 2015; Vigier et al., 2008), although compilations suggest there
327 should still be significant Li isotope fractionation at 300–350°C (Marschall et al.,
328 2007). Therefore, in these hydrothermal springs, higher temperatures appear to
329 promote more congruent weathering (corresponding to higher dissolution rates
330 (Stefansson et al., 2001)), accounting for the higher elemental concentrations in

331 warmer waters. This applies to elements such as the alkali metals (Li, Na, K), but
332 not for elements such as Mg or Fe, which are trace elements in geothermal
333 waters (Albarede and Michard, 1986; Elderfield and Schultz, 1996; Holland,
334 2005), as also shown by a positive co-variation of Mg/Na and Li isotopes (not
335 shown), where low Mg/Na ratios coincide with low $\delta^7\text{Li}$ and high temperatures.

336 A general weathering (primary mineral dissolution vs. secondary mineral
337 formation) control on Li is confirmed by a negative co-variation between $\delta^7\text{Li}$
338 and conductivity (Fig. 3). Effectively, the more minerals that are dissolving
339 and/or the less cations that are being retained in secondary minerals (relative to
340 those provided by dissolution), the higher the conductivity (and individual
341 elemental concentrations). In turn, the higher conductivity is, the more cations
342 will eventually be washed into the oceans. Thus, a higher conductivity (itself
343 caused by greater total dissolved solids) is a function of more efficient silicate
344 weathering, in that relatively less material is being sequestered into secondary
345 minerals (i.e. greater primary mineral dissolution or less secondary mineral
346 formation). The relationship between Li isotopes and secondary minerals
347 formation has therefore led to the suggestion that $\delta^7\text{Li}$ is a tracer for the silicate
348 weathering efficiency (Pogge von Strandmann and Henderson, 2015). The
349 relatively less cations (mainly Ca and Mg) that are retained in secondary
350 minerals, the more efficient chemical weathering will be at transporting cations
351 to the oceans, where they will allow carbonate precipitation, and therefore,
352 eventually, CO₂ sequestration (Pogge von Strandmann and Henderson, 2015).

353 The possibility of using $\delta^7\text{Li}$ to trace overall weathering and CO₂
354 drawdown efficiency depends on whether the behaviour of Li in the weathering
355 environment is similar to the elements implicated in carbonate formation,
356 primarily Ca and Mg. In basaltic rivers, the mobility relative to the most mobile
357 cation, Na (where relative mobility = $[\text{X}_{\text{dissolved}}/\text{Na}_{\text{dissolved}}]/[\text{X}_{\text{rock}}/\text{Na}_{\text{rock}}]$ (Gíslason
358 et al., 1996)), can be calculated. It must be stressed that there are some
359 secondary minerals in Iceland (principally zeolites) that can take up Na, although
360 these are generally observed to only form at hundreds of metres basalt depth
361 (Alfredsson et al., 2013)). In Icelandic rivers, Ca is on average $3.6^{+3.8}_{-1.7}$ times more
362 mobile than Li (Pogge von Strandmann et al., 2006). Catchments with a high

363 degree of glaciation (i.e. significant supply of fine-grained, fresh, primary
364 material) exhibit close-to-identical Ca and Li mobility, whereas in older
365 catchments, Ca is more mobile than Li. In the Azores, Ca is on average 4.2 times
366 more mobile than Li (Pogge von Strandmann et al., 2010), while in Reunion, this
367 value is 3.1 (Louvat and Allegre, 1997). Overall, this suggests that in basaltic
368 rivers, Li is 3–4 times less mobile than Ca. This relative similarity is also
369 demonstrated by correlations between Li and Ca isotopes in Icelandic rivers
370 (Hindshaw et al., 2013). Similarly, in Icelandic rivers, Mg is $1.6^{+2.3}_{-0.8}$ times more
371 mobile than Li, and Si is $1.2^{+2.4}_{-0.5}$ times more mobile (Pogge von Strandmann et al.,
372 2006). Overall, therefore, this means that Li is one of the trace elements with the
373 closest relative mobility to these three key elements (trace elements such as Fe,
374 Al or Mn are orders of magnitude less mobile (Gíslason et al., 1996)), and
375 therefore this suggests that in some rivers Li isotopes are a useful tracer of
376 silicate weathering efficiency, and hence CO₂ drawdown efficiency (supported by
377 a correlation between $\delta^7\text{Li}$ and Ca isotopes (Hindshaw et al., 2013)). However, in
378 hydrothermal springs, which can be a major source of cations to rivers in many
379 basaltic catchments, especially in ocean islands or arc settings, elemental
380 mobility is different. In the Myvatn springs, Ca is on average 0.4 times as mobile
381 as Li in low temperature springs, and 0.1 times as mobile in high temperature
382 springs. Similarly, Mg is 0.3 times as mobile in low temperature, and 0.04 times
383 as mobile in high temperature springs as Li. Hence, the apparent mobility of Li
384 will increase in rivers with hydrothermal sources, meaning that such rivers must
385 be corrected for before Li isotopes can be used as meaningful weathering tracers.

386 This utility of Li isotopes as a tracer of secondary mineral formation
387 processes is also highlighted by co-variations between $\delta^7\text{Li}$ and several different
388 elemental ratio tracers of weathering processes. A recent study of weathering of
389 the Columbia River Basalts has proposed Li/Na ratios as another tracer that, like
390 $\delta^7\text{Li}$, is sensitive to the degree of water-rock interaction over time (Liu et al.,
391 2015). Reactive transport models suggest that Li/Na increases with decreasing
392 residence time, while $\delta^7\text{Li}$ decreases (Liu et al., 2015). This model is supported
393 both by published basaltic terrain data (Liu et al., 2015; Pogge von Strandmann
394 et al., 2010; Pogge von Strandmann et al., 2006; Vigier et al., 2009) and this study

395 (Fig. 4), and can be explained as reflecting incorporation of Li into secondary
396 minerals (assisted by less isotopic fractionation at high temperatures), while Na
397 is highly mobile and present in greater proportion, and is not affected to the
398 same degree by secondary mineral formation.

399 Equally, Myvatn spring $\delta^7\text{Li}$ co-varies with another proposed tracer of
400 weathering intensity, $\text{K}/(\text{Na}+\text{K})$, where high values reflect supply-limited
401 weathering, and low values reflect kinetic-limited reactions (Edmond et al.,
402 1995; Pogge von Strandmann et al., 2010; Stallard and Edmond, 1983; Stallard
403 and Edmond, 1987). As in the basaltic Azores (Pogge von Strandmann et al.,
404 2010), these samples exhibit a negative relationship between $\text{K}/(\text{Na}+\text{K})$ and $\delta^7\text{Li}$
405 (Fig. 4). Although several studies have demonstrated that the overall relationship
406 between Li isotopes and weathering regime is more complex than a linear
407 relationship, especially in lithologically complex terrains, and likely reflects an
408 inverse bell-shaped curve, due to leaching of light secondary clays (Bouchez et
409 al., 2013; Dellinger et al., 2015), it is not surprising that in a simple weathering
410 regime like Iceland or the Azores such a relationship is linear, because
411 dissolution of previously formed secondary minerals is unlikely to have a
412 significant influence on Li isotopes. Hence, in a kinetic-limited regime, as defined
413 by low $\text{K}/(\text{Na}+\text{K})$, with short residence times, $\delta^7\text{Li}$ values are low, and vice versa
414 in supply-limited regimes (Bouchez et al., 2013; Dellinger et al., 2015; Pogge von
415 Strandmann et al., 2010).

416 Finally, the effect of clay mineral formation on Li isotopes can be tested by
417 comparing solution $\delta^7\text{Li}$ with the ratio of a mobile to an immobile element, such
418 as Na/Ti or Na/Al (Fig 4a). Such a ratio should in principle behave in the same
419 manner as Li isotopes in a monolithologic environment, because it should
420 respond to mineral dissolution relative to clay formation. This is demonstrated
421 by a negative relationship between Na/Ti and $\delta^7\text{Li}$ (Fig. 4 – a similar relationship
422 for Na/Al is not shown). Combined, these elemental relationships confirm that
423 even in hydrothermal groundwaters, Li isotopes are controlled by the same
424 processes that are thought to control their behaviour in river systems: the ratio
425 of primary mineral dissolution to secondary mineral formation, which has
426 variously been termed weathering intensity, weathering congruency or
427 weathering efficiency (Dellinger et al., 2015; Misra and Froelich, 2012; Pogge von

428 Strandmann et al., 2010; Pogge von Strandmann and Henderson, 2015; Pogge
429 von Strandmann et al., 2013). However, in contrast to rivers, the key controlling
430 process of weathering intensity is temperature rather than interaction time, and
431 its effect on inhibiting secondary mineral formation, promoting fully congruent
432 weathering at high temperatures. Isotopic fractionation factors are also less at
433 these higher temperatures, although it is likely that around 5–6‰ $\delta^7\text{Li}$ would
434 still occur if secondary minerals were abundantly present (Marschall et al.,
435 2007).

436

437 5.1.2 Comparison to Si isotopes as a weathering tracer

438 Silicon isotope ratios have also been determined in these samples
439 (Opfergelt et al., 2011). In theory, $\delta^{30}\text{Si}$ behaves similarly to $\delta^7\text{Li}$, in that both
440 systems are used as silicate weathering tracers, where secondary minerals
441 preferentially take up light isotopes, driving river waters and seawater to
442 isotopically heavy values (De la Rocha et al., 2000; Georg et al., 2006; Georg et al.,
443 2007; Opfergelt et al., 2013; Opfergelt et al., 2009; Ziegler et al., 2005). In
444 addition, for Si isotopes, biology and plant growth exerts an influence, and
445 preferentially take up light isotopes (Opfergelt et al., 2006). The mobility of Si in
446 Icelandic river waters is $1.2^{+2.4}_{-0.5}$ times as mobile as Li (Pogge von Strandmann et
447 al., 2006), again suggesting the two systems might have similar weathering
448 behaviour in rivers. In contrast, in the Myvatn springs, Si is approximately $0.2 \pm$
449 0.1 times as mobile as Li. Silicon isotope ratios in these groundwaters are heavier
450 than the host basalt or basaltic soils, but are within the range exhibited by
451 Icelandic soil pore waters (Pogge von Strandmann et al., 2012), suggesting that
452 weathering processes also dominate the Si budget here (Fig. 5). However, $\delta^{30}\text{Si}$ in
453 these groundwaters is fairly uniform (0.35–0.62‰), and shows no co-variation
454 with $\delta^7\text{Li}$ or any of the factors that appear to influence the Li isotope ratio of
455 these waters. A lack of co-variation between Li and Si isotopes has been
456 observed before in the weathering environment (Georg et al., 2007; Pogge von
457 Strandmann et al., 2012; Pogge von Strandmann et al., 2014b; Vigier et al., 2009),
458 and generally implies that the behaviour of Si, an element that is a major
459 component of rocks and secondary minerals, is quite different from that of a

460 minor element, such as Li, that adsorbs to mineral surfaces and substitutes into
461 mineral lattices. Thus, the $\delta^{30}\text{Si}$ variation in these springs is considerably less
462 than that observed in Icelandic rivers or soil pore waters, while the $\delta^7\text{Li}$
463 variability in all three phases is similar.

464 Given that it is unlikely that biology plays a significant role in these
465 springs, it is possible that the increased $\delta^{30}\text{Si}$ variability in rivers and pore waters
466 relative to these springs is due to Si utilisation by plants or diatoms in the
467 river/pore waters. However, it has been demonstrated that $\delta^{30}\text{Si}$ in Icelandic soil
468 pore waters in a relatively plant-rich area is controlled by silicate weathering
469 processes, rather than biology (Pogge von Strandmann et al., 2012), which
470 suggests overall plants do not control Si isotopes in Icelandic environments.

471 There are no co-variations between Si isotope ratios and secondary
472 mineral saturation states, and virtually no correlations for Li isotope ratios,
473 which suggests that the effects of a series of different precipitating minerals are
474 entangled. Both isotope systems are also affected by adsorption onto minerals
475 with no Si component, such as Fe oxyhydroxides (Delstanche et al., 2009).
476 However, the fractionation factors for both systems are known (Delstanche et al.,
477 2009; Millot and Girard, 2007; Pistiner and Henderson, 2003; Pogge von
478 Strandmann et al., 2012), and would not account for large $\delta^7\text{Li}$ variability with
479 little $\delta^{30}\text{Si}$ fractionation. This therefore suggests that the reaction kinetics of the
480 two isotope systems are distinctly different. Lithium has been shown to diffuse
481 on the cm scale extremely quickly (on the order of minutes) at temperatures of
482 75°C in aqueous solutions up to magmatic temperatures in silicates (Richter et
483 al., 2003; Richter et al., 2006; Teng et al., 2010). Hence, it seems likely that the
484 water-rock interaction time of these springs provides sufficient time for
485 significant Li isotope fractionation, but not for Si isotope fractionation, if the
486 reaction remains kinetic. In contrast, soil pore waters provide sufficient water-
487 rock interaction time for Si isotope fractionation to occur as well as Li, and these
488 fractionations are inherited by river waters.

489

490 *5.2 Outflow (Laxa River) time series*

491 The key aspect of Myvatn is that it is a very productive lake, which is also
492 lined with high Si, low Al diatomaceous sediments, which inhibit Al-silicate clay

493 formation in the lake. Given Iceland's latitude, the lake's productivity is strongly
494 seasonal. The Laxa River is the only outflow from the lake, and therefore a time
495 series taken from this river shows that the concentration of most elements is
496 also strongly seasonal. Nutrients such as NO_3 are more concentrated in the
497 winter, and less in the summer, when they are being utilised in primary
498 productivity by diatoms, algae and cyanobacteria. Other bio-utilised elements
499 (Na, K, Fe, etc.) are similarly affected. In particular, Si concentrations are around
500 eight times higher in the winter than the summer, due to diatom growth
501 (Opfergelt et al., 2011). This also has a strong affect on Si isotopes, which
502 characterise two diatom blooms that drive lake water $\delta^{30}\text{Si} \sim 0.7\text{‰}$ higher in the
503 summer.

504 The effect of the change in productivity on elemental concentrations is
505 also reflected in calculations of mineral stability, although it is difficult to
506 ascertain whether the saturation of both primary and secondary mineral is truly
507 affected, or whether biology dominates elemental concentrations. In any case,
508 lithium is the only element of those measured that is completely unaffected by
509 the changes in productivity during the year. Lithium concentrations show no
510 trend with time whatsoever (Fig. 6), although they do exhibit some non-
511 systematic variation, which is likely due to relative variations in the groundwater
512 spring input into Myvatn. Equally, Li isotope ratios are unaffected by changes in
513 primary productivity. There is no trend of $\delta^7\text{Li}$ with time (slightly higher $\delta^7\text{Li}$
514 values in spring 2001 did not occur in spring 2000), and the $\sim 3.7\text{‰}$ variation
515 within the Laxa River time series is very small, especially when compared to
516 almost 40‰ variation observed in all rivers draining basaltic terrains (Liu et al.,
517 2015; Pogge von Strandmann et al., 2010; Pogge von Strandmann et al., 2006;
518 Vigier et al., 2009).

519 This lack of $\delta^7\text{Li}$ change provides a very strong indication that Li does not
520 behave as a nutrient used in primary productivity. It has been suggested that Li
521 isotopes are not affected by plant growth (Lemarchand et al., 2010), but this is
522 the first test that demonstrates that primary phytoplankton productivity is also
523 not a factor in affecting Li isotope ratios. As a consequence Li has a significant
524 advantage over other weathering tracers, especially the major elements (e.g. Mg,
525 Si, Ca isotopes), which are demonstrably affected by biological processes (Black

526 et al., 2006; Bolou-Bi et al., 2010; Bolou-Bi et al., 2012; Fantle and Tipper, 2014;
527 Opfergelt et al., 2010; Opfergelt et al., 2011; Pogge von Strandmann, 2008; Pogge
528 von Strandmann et al., 2014a). This, therefore, enhances the potential role of Li
529 isotopes as the only tracer that solely responds to silicate weathering processes,
530 and is unaffected by biological processes or carbonate weathering.

531

532 6.0 Conclusions

533 This study has analysed Li isotopes in the hydrothermal springs that are
534 the dominant source of cations to Lake Myvatn, as well as a time series for the
535 Laxa River, the only point of outflow from the lake.

536 Lithium isotope ratios in the high- and low-temperature springs co-vary
537 with temperature. High-temperature springs ($\leq 44^\circ\text{C}$) have similar $\delta^7\text{Li}$ to
538 continental and marine basaltic hydrothermal systems measured at $\sim 350^\circ\text{C}$,
539 implying that secondary mineral precipitation (inhibited at high temperatures)
540 has not occurred during cooling as these waters migrated towards Myvatn from
541 the Krafla geothermal field. Isotope fractionation during secondary mineral
542 precipitation was also likely lower at these higher temperatures, although
543 probably still substantial enough to have caused an observable effect if the
544 minerals were present. In contrast, low-temperature groundwaters exhibit
545 significant $\delta^7\text{Li}$ fractionation due to secondary mineral formation.

546 Co-variations between $\delta^7\text{Li}$ and a series of elemental tracers of
547 weathering processes (Li/Na, K/(Na+K), etc.) show that $\delta^7\text{Li}$ in these springs is
548 controlled by the same processes that affect Li in rivers and groundwaters: the
549 ratio of primary rock dissolution to secondary mineral formation (termed the
550 weathering intensity, weathering congruency or weathering efficiency). Thus,
551 weathering is highly congruent in the high-temperature springs (partly assisted
552 by lower isotopic fractionation factors), and incongruent in low-temperature
553 groundwaters. Hence, Li isotope signals in river waters can be strongly
554 influenced by hydrothermal input, because waters that have had high water-rock
555 interaction (which causes high Li isotope fractionation at low temperatures) at
556 high temperatures will still have unfractionated Li isotope ratios. Interestingly,
557 in the same springs, Si isotope ratios are relatively constant, highlighting the

558 difference in reaction time and kinetic activity between these two purported
559 silicate weathering tracers.

560 In contrast, while $\delta^{30}\text{Si}$ exhibit strong seasonal variations, the time series
561 outflow in the Laxa River exhibits little $\delta^7\text{Li}$ variation. Myvatn has extremely high
562 seasonal primary productivity, which strongly affects most elements, as well as
563 Si isotopes. However, [Li] and $\delta^7\text{Li}$ are unaffected by these productivity changes.
564 This provides some of the strongest evidence yet reported that Li isotopes are
565 not affected by plant growth or biology, meaning that Li isotopes remain the
566 most useful tracer of solely silicate weathering processes available.

567

568 Acknowledgements

569 Analyses and PPvS were funded by NERC Research Fellowship NE/I020571/2.
570 We thank Josh Wimpenny, Xiao-Ming Liu and an anonymous reviewer for their
571 useful reviews.

572

- 573 Albarede, F., Michard, A., 1986. Transfer of Continental Mg, S, O and U to the
574 Mantle through Hydrothermal Alteration of the Oceanic-Crust. *Chemical*
575 *Geology*, 57(1-2): 1-15.
- 576 Alfredsson, H.A. et al., 2013. The geology and water chemistry of the Hellisheidi,
577 SW-Iceland carbon storage site. *International Journal of Greenhouse Gas*
578 *Control*, 12: 399–418.
- 579 Allegre, C.J. et al., 2010. The fundamental role of island arc weathering in the
580 oceanic Sr isotope budget. *Earth and Planetary Science Letters*, 292(1-2):
581 51-56.
- 582 Archer, D., Winguth, A., Lea, D.W., Mahowald, N., 2000. What causes the
583 glacial/interglacial atmospheric $p\text{CO}_2$ cycles? *Reviews of Geophysics*, 38:
584 159-189.
- 585 Bagard, M.-L., West, A.J., Newman, K., Basu, A.K., 2015. Lithium isotope
586 fractionation in the Ganges–Brahmaputra floodplain and implications for
587 groundwater impact on seawater isotopic composition. *Earth and*
588 *Planetary Science Letters*, 432: 404–414.
- 589 Berner, R.A., 2003. The long-term carbon cycle, fossil fuels and atmospheric
590 composition. *Nature*, 426(6964): 323-326.
- 591 Black, J.R., Yin, Q.Z., Casey, W.H., 2006. An experimental study of magnesium-
592 isotope fractionation in chlorophyll-a photosynthesis. *Geochimica Et*
593 *Cosmochimica Acta*, 70(16): 4072-4079.
- 594 Blum, J.D., Erel, Y., 1997. Rb-Sr isotope systematics of a granitic soil
595 chronosequence: The importance of biotite weathering. *Geochimica Et*
596 *Cosmochimica Acta*, 61(15): 3193-3204.

597 Bodvarsson, G.S., Pruess, K., Stefansson, V., Eliasson, E.T., 1984. The Krafla
598 Geothermal Field, Iceland. 2. The Natural State of the System. *Water*
599 *Resources Research*, 20(11): 1531–1544.

600 Bolou-Bi, E.B., Poszwa, A., Leyval, C., Vigier, N., 2010. Experimental determination
601 of magnesium isotope fractionation during higher plant growth.
602 *Geochimica Et Cosmochimica Acta*, 74(9): 2523-2537.

603 Bolou-Bi, E.B., Vigier, N., Poszwa, A., Boudot, J.-P., Dambrine, E., 2012. Effects of
604 biogeochemical processes on magnesium isotope variations in a forested
605 catchment in the Vosges Mountains (France). *Geochimica Et*
606 *Cosmochimica Acta*, 87: 341–355.

607 Bouchez, J., von Blanckenburg, F., Schuessler, J.A., 2013. Modeling novel stable
608 isotope ratios in the weathering zone. *American Journal of Science*, 313.

609 Chan, L.H., Edmond, J.M., Thompson, G., 1993. A lithium isotope study of hot
610 springs and metabasalts from mid-ocean ridge hydrothermal systems.
611 *Journal of Geophysical Research*, 98: 9653-9659.

612 Chan, L.H., Gieskes, J.M., You, C.F., Edmond, J.M., 1994. Lithium isotope
613 geochemistry of sediments and hydrothermal fluids of the Guaymas
614 Basin, Gulk of California. *Geochimica Et Cosmochimica Acta*, 58: 4443-
615 4454.

616 De la Rocha, C.L., Brzezinski, M.A., DeNiro, M.J., 2000. A first look at the
617 distribution of the stable isotopes of silicon in natural waters. *Geochimica*
618 *Et Cosmochimica Acta*, 64(14): 2467-2477.

619 Dellinger, M. et al., 2014. Lithium isotopes in large rivers reveal the cannibalistic
620 nature of modern continental weathering and erosion. *Earth and*
621 *Planetary Science Letters*, 401: 359–372.

622 Dellinger, M. et al., 2015. Riverine Li isotope fractionation in the Amazon River
623 basin controlled by the weathering regimes. *Geochimica Et Cosmochimica*
624 *Acta*, 164: 71–93.

625 Delstanche, S. et al., 2009. Silicon isotopic fractionation during adsorption of
626 aqueous monosilicic acid onto iron oxide. *Geochimica Et Cosmochimica*
627 *Acta*, 73: 923-934.

628 Dessert, C., Dupre, B., Gaillardet, J., Francois, L.M., Allegre, C.J., 2003. Basalt
629 weathering laws and the impact of basalt weathering on the global carbon
630 cycle. *Chemical Geology*, 202(3-4): 257–273.

631 Edmond, J.M., Palmer, M.R., Measures, C.I., Grant, B., Stallard, R.F., 1995. The
632 Fluvial Geochemistry and Denudation Rate of the Guayana Shield in
633 Venezuela, Colombia, and Brazil. *Geochimica Et Cosmochimica Acta*,
634 59(16): 3301-3325.

635 Elderfield, H., Schultz, A., 1996. Mid-ocean ridge hydrothermal fluxes and the
636 chemical composition of the ocean. *Annual Review of Earth and Planetary*
637 *Sciences*, 24: 191-224.

638 Elliott, T., Thomas, A., Jeffcoate, A., Niu, Y.L., 2006. Lithium isotope evidence for
639 subduction-enriched mantle in the source of mid-ocean-ridge basalts.
640 *Nature*, 443(7111): 565–568.

641 Fantle, M.S., Tipper, E.T., 2014. Calcium isotopes in the global biogeochemical Ca
642 cycle: Implications for development of a Ca isotope proxy. *Earth-Science*
643 *Reviews*, 129: 148–177.

644 Flesch, G.D., Anderson, A.R., Svec, H.J., 1973. A secondary isotopic standard for
645 $^6\text{Li}/^7\text{Li}$ determinations. *Int. J. Mass Spectrom. Ion Process.*, 12: 265–272.

646 Gaillardet, J., Dupre, B., Louvat, P., Allegre, C.J., 1999. Global silicate weathering
647 and CO₂ consumption rates deduced from the chemistry of large rivers.
648 *Chemical Geology*, 159(1-4): 3-30.

649 Georg, R.B., Reynolds, B.C., Frank, M., Halliday, A.N., 2006. Mechanisms
650 controlling the silicon isotopic compositions of river waters. *Earth and*
651 *Planetary Science Letters*, 249(3-4): 290-306.

652 Georg, R.B., Reynolds, B.C., West, A.J., Burton, K.W., Halliday, A.N., 2007. Silicon
653 isotope variations accompanying basalt weathering in Iceland. *Earth and*
654 *Planetary Science Letters*, 261: 476-490.

655 Gislason, S.R., 2005. Chemical weathering, chemical denudation and the CO₂
656 budget for Iceland. In: Caseldine, C.J., Russell, A., Hardardóttir, J., Knudsen,
657 O. (Eds.), *Iceland: Modern processes, Past Environments*. Elsevier, pp.
658 289-307.

659 Gíslason, S.R., Arnorsson, S., Armannsson, H., 1996. Chemical weathering of
660 basalt in southwest Iceland: Effects of runoff, age of rocks and
661 vegetative/glacial cover. *American Journal of Science*, 296(8): 837-907.

662 Gislason, S.R., Eiriksdottir, E.S., Olafsson, J., 2004. Chemical composition of
663 interstitial water and diffusive fluxes within the diatomaceous sediment
664 in Lake Myvatn, Iceland. *Aquatic Ecology*, 38: 163-175.

665 Gislason, S.R. et al., 2009. Direct evidence of the feedback between climate and
666 weathering. *Earth and Planetary Science Letters*, 277(1-2): 213-222.

667 Hall, J.M., Chan, L.H., McDonough, W.F., Turekian, K.K., 2005. Determination of the
668 lithium isotopic composition of planktic foraminifera and its application
669 as a paleo-seawater proxy. *Marine Geology*, 217(3-4): 255-265.

670 Hathorne, E.C., James, R.H., 2006. Temporal record of lithium in seawater: a
671 tracer for silicate weathering? *Earth and Planetary Science Letters*, 246:
672 393-406.

673 Hauptfleisch, U., Einarsson, A., 2012. Age of the Younger Laxá Lava and Lake
674 Myvatn, northern Iceland, determined by AMS Radiocarbon Dating.
675 *Radiocarbon*, 54: 155-164.

676 Henchiri, S. et al., 2014. The influence of hydrothermal activity on the Li isotopic
677 signature of rivers draining volcanic areas. *Procedia Earth and Planetary*
678 *Science*, 10: 223-230.

679 Henley, R.W., Ellis, A.J., 1983. Geothermal Systems Ancient and Modern: A
680 *Geochemical Review*. *Earth-Science Reviews*, 19: 1-50.

681 Hindshaw, R.S., Bourdon, B., Pogge von Strandmann, P.A.E., Vigier, N., Burton,
682 K.W., 2013. The stable calcium isotopic composition of rivers draining
683 basaltic catchments in Iceland. *Earth and Planetary Science Letters*, 374:
684 173-184.

685 Hoefs, J., Sywall, M., 1997. Lithium isotope composition of Quaternary and
686 Tertiary biogenic carbonates and a global lithium isotope balance.
687 *Geochimica Et Cosmochimica Acta*, 61(13): 2679-2690.

688 Hogan, J.F., Blum, J.D., 2003. Boron and lithium isotopes as groundwater tracers:
689 a study at the Fresh Kills Landfill, Staten Island, New York, USA. *Applied*
690 *Geochemistry*, 18(4): 615-627.

691 Holland, H.D., 2005. Sea level, sediments and the composition of seawater.
692 *American Journal of Science*, 305: 220-239.

693 Huh, Y., Chan, L.H., Edmond, J.M., 2001. Lithium isotopes as a probe of weathering
694 processes: Orinoco River. *Earth and Planetary Science Letters*, 194(1-2):
695 189–199.

696 Huh, Y., Chan, L.H., Zhang, L., Edmond, J.M., 1998. Lithium and its isotopes in
697 major world rivers: Implications for weathering and the oceanic budget.
698 *Geochimica Et Cosmochimica Acta*, 62(12): 2039–2051.

699 Jones, C.E., Jenkyns, H.C., 2001. Seawater strontium isotopes, oceanic anoxic
700 events, and seafloor hydrothermal activity in the Jurassic and Cretaceous.
701 *American Journal of Science*, 301(2): 112–149.

702 Kiskurek, B., James, R.H., Harris, N.B.W., 2005. Li and $\delta^7\text{Li}$ in Himalayan rivers:
703 Proxies for silicate weathering? *Earth and Planetary Science Letters*,
704 237(3-4): 387–401.

705 Kristmannsdottir, H.K., Armannsson, H., 2004. Groundwater in the Lake Myvatn
706 area, North Iceland: chemistry, origin and interaction. *Aquatic Ecology*,
707 38: 115–128.

708 Lechler, M., Pogge von Strandmann, P.A.E., Jenkyns, H.C., Prosser, G., Parente, M.,
709 2015. Lithium-isotope evidence for enhanced silicate weathering during
710 OAE 1a (Early Aptian Selli event). *Earth and Planetary Science Letters*,
711 432: 210–222.

712 Lemarchand, E., Chabaux, F., Vigier, N., Millot, R., Pierret, M.C., 2010. Lithium
713 isotope systematics in a forested granitic catchment (Strengbach, Vosges
714 Mountains, France). *Geochimica Et Cosmochimica Acta*, 74: 4612-4628.

715 Liu, X.-M., Wanner, C., Rudnick, R.L., McDonough, W.F., 2015. Processes
716 controlling $\delta^7\text{Li}$ in rivers illuminated by study of streams and
717 groundwaters draining basalts. *Earth and Planetary Science Letters*, 409:
718 212–224.

719 Louvat, P., Allegre, C.J., 1997. Present denudation rates on the island of Reunion
720 determined by river geochemistry: Basalt weathering and mass budget
721 between chemical and mechanical erosions. *Geochimica Et Cosmochimica*
722 *Acta*, 61(17): 3645-3669.

723 Louvat, P., Gislason, S.R., Allegre, C.J., 2008. Chemical and mechanical erosion
724 rates in Iceland as deduced from river dissolved and solid material.
725 *American Journal of Science*, 308: 679-726.

726 Marschall, H.R., Pogge von Strandmann, P.A.E., Seitz, H.M., Elliott, T., Niu, Y.L.,
727 2007. The lithium isotopic composition of orogenic eclogites and deep
728 subducted slabs. *Earth and Planetary Science Letters*, 262: 563-580.

729 Meredith, K., Moriguti, T., Tomascak, P., Hollins, S., Nakamura, E., 2013. The
730 lithium, boron and strontium isotopic systematics of groundwaters from
731 an arid aquifer system: Implications for recharge and weathering
732 processes. *Geochimica Et Cosmochimica Acta*, 112: 20–31.

733 Millot, R., Girard, J.P., 2007. Lithium Isotope Fractionation during adsorption
734 onto mineral surfaces, International meeting, Clays in natural &
735 engineered barriers for radioactive waste confinement, Lille, France.

736 Millot, R., Scaillet, B., Sanjuan, B., 2010a. Lithium isotopes in island arc
737 geothermal systems: Guadeloupe, Martinique (French West Indies) and
738 experimental approach. *Geochimica Et Cosmochimica Acta*, 74(6): 1852-
739 1871.

740 Millot, R., Vigier, N., Gaillardet, J., 2010b. Behaviour of lithium and its isotopes
741 during weathering in the Mackenzie Basin, Canada. *Geochimica Et*
742 *Cosmochimica Acta*, 74: 3897–3912.

743 Misra, S., Froelich, P.N., 2012. Lithium Isotope History of Cenozoic Seawater:
744 Changes in Silicate Weathering and Reverse Weathering. *Science*, 335:
745 818–823.

746 Negrel, P., Millot, R., Brenot, A., Bertin, C., 2010. Lithium isotopes as tracers of
747 groundwater circulation in a peat land. *Chemical Geology*, 276: 119-127.

748 Negrel, P. et al., 2012. Heterogeneities and interconnections in groundwaters:
749 Coupled B, Li and stable-isotope variations in a large aquifer system
750 (Eocene Sand aquifer, Southwestern France). *Chemical Geology*, 296-297:
751 83-95.

752 Olafsson, J., 1979. Physical characteristics of Lake Myvatn and River Laxá. *Oikos*,
753 32: 38–66.

754 Oliver, L. et al., 2003. Silicate weathering rates decoupled from the $^{87}\text{Sr}/^{86}\text{Sr}$ ratio
755 of the dissolved load during Himalayan erosion. *Chemical Geology*, 201(1-
756 2): 119–139.

757 Opfergelt, S., Burton, K.W., Pogge von Strandmann, P.A.E., Gislason, S.R., Halliday,
758 A.N., 2013. Riverine silicon isotope variations in glaciated basaltic
759 terrains: Implications for the Si delivery to the ocean over glacial–
760 interglacial intervals. *Earth and Planetary Science Letters*, 369–370: 211–
761 219.

762 Opfergelt, S. et al., 2010. Variations of $\delta^{30}\text{Si}$ and Ge/Si With Weathering and
763 Biogenic Input in Tropical Basaltic Ash Soils Under Monoculture.
764 *Geochimica Et Cosmochimica Acta*, 74: 225-240.

765 Opfergelt, S. et al., 2006. Silicon Isotopic Fractionation by Banana (*Musa spp.*)
766 Grown in a Continuous Nutrient Flow Device. *Plant Soil*, 285: 333-345.

767 Opfergelt, S. et al., 2009. Impact of soil weathering degree on silicon isotopic
768 fractionation during adsorption onto iron oxides in basaltic ash soils,
769 Cameroon. *Geochimica Et Cosmochimica Acta*, 73: 7226-7240.

770 Opfergelt, S. et al., 2011. Quantifying the impact of freshwater diatom
771 productivity on silicon isotopes and silicon fluxes: Lake Myvatn, Iceland.
772 *Earth and Planetary Science Letters*, 305(1-2): 73-82.

773 Palmer, M.R., Edmond, J.M., 1992. Controls over the strontium isotope
774 composition of river water. *Geochimica Et Cosmochimica Acta*, 56(5):
775 2099-2111.

776 Parkhurst, D.L., Appelo, C.A.J., 1999. User's guide to PHREEQC (version 2) - a
777 computer program for speciation, batch-reaction, one-dimensional
778 transport, and inverse geochemical calculations.

779 Pistiner, J.S., Henderson, G.M., 2003. Lithium-isotope fractionation during
780 continental weathering processes. *Earth and Planetary Science Letters*,
781 214(1-2): 327-339.

782 Pogge von Strandmann, P.A.E., 2008. Precise magnesium isotope measurements
783 in core top planktic and benthic foraminifera. *Geochemistry Geophysics*
784 *Geosystems*, 9(12): Q12015.

785 Pogge von Strandmann, P.A.E., Burton, K.W., James, R.H., van Calsteren, P.,
786 Gislason, S.R., 2008a. The influence of weathering processes on riverine
787 magnesium isotopes in a basaltic terrain. *Earth and Planetary Science*
788 *Letters*, 276: 187-197.

789 Pogge von Strandmann, P.A.E., Burton, K.W., James, R.H., van Calsteren, P.,
790 Gislason, S.R., 2010. Assessing the role of climate on uranium and lithium
791 isotope behaviour in rivers draining a basaltic terrain. *Chemical Geology*,
792 270: 227–239.

793 Pogge von Strandmann, P.A.E. et al., 2006. Riverine behaviour of uranium and
794 lithium isotopes in an actively glaciated basaltic terrain. *Earth and
795 Planetary Science Letters*, 251: 134–147.

796 Pogge von Strandmann, P.A.E. et al., 2011. Variations of Li and Mg isotope ratios
797 in bulk chondrites and mantle xenoliths. *Geochimica Et Cosmochimica
798 Acta*, 75: 5247–5268.

799 Pogge von Strandmann, P.A.E., Forshaw, J., Schmidt, D.N., 2014a. Modern and
800 Cenozoic records of seawater magnesium from foraminiferal Mg isotopes.
801 *Biogeosciences*, 11: 5155–5168.

802 Pogge von Strandmann, P.A.E., Henderson, G.M., 2015. The Li isotope response to
803 mountain uplift. *Geology*, 43(1): 67–70.

804 Pogge von Strandmann, P.A.E., James, R.H., van Calsteren, P., Gíslason, S.R.,
805 Burton, K.W., 2008b. Lithium, magnesium and uranium isotope behaviour
806 in the estuarine environment of basaltic islands. *Earth and Planetary
807 Science Letters*, 274(3-4): 462-471.

808 Pogge von Strandmann, P.A.E., Jenkyns, H.C., Woodfine, R.G., 2013. Lithium
809 isotope evidence for enhanced weathering during Oceanic Anoxic Event 2.
810 *Nature Geoscience*, 6: 668–672.

811 Pogge von Strandmann, P.A.E. et al., 2012. Lithium, magnesium and silicon
812 isotope behaviour accompanying weathering in a basaltic soil and pore
813 water profile in Iceland. *Earth and Planetary Science Letters*, 339–340:
814 11–23.

815 Pogge von Strandmann, P.A.E. et al., 2014b. Chemical weathering processes in
816 the Great Artesian Basin: Evidence from lithium and silicon isotopes.
817 *Earth and Planetary Science Letters*, 406: 24–36.

818 Rad, S., Rive, K., Vittecoq, B., Cerdan, O., Allegre, C.J., 2013. Chemical weathering
819 and erosion rates in the Lesser Antilles: An overview in Guadeloupe,
820 Martinique and Dominica. *Journal of South American Earth Sciences*, 45:
821 331-344.

822 Raymo, M.E., Ruddiman, W.F., Froelich, P.N., 1988. Influence of late Cenozoic
823 mountain building on ocean geochemical cycles *Geology*, 16: 649-653.

824 Richter, F.M., Davis, A.M., DePaolo, D.J., Watson, E.B., 2003. Isotope fractionation
825 by chemical diffusion between molten basalt and rhyolite. *Geochimica Et
826 Cosmochimica Acta*, 67(20): 3905-3923.

827 Richter, F.M. et al., 2006. Kinetic isotopic fractionation during diffusion of ionic
828 species in water. *Geochimica Et Cosmochimica Acta*, 70: 277-289.

829 Sauzeat, L., Rudnick, R.L., Chauvel, C., Garçon, M., Tang, M., 2015. New
830 perspectives on the Li isotopic composition of the upper continental crust
831 and its weathering signature. *Earth and Planetary Science Letters*, 428:
832 181–192.

833 Stallard, R.F., Edmond, J.M., 1983. Geochemistry of the Amazon .2. The Influence
834 of Geology and Weathering Environment on the Dissolved-Load. *Journal
835 of Geophysical Research-Oceans and Atmospheres*, 88(NC14): 9671-9688.

836 Stallard, R.F., Edmond, J.M., 1987. Geochemistry of the Amazon .3. Weathering
837 Chemistry and Limits to Dissolved Inputs. *Journal of Geophysical*
838 *Research-Oceans*, 92(C8): 8293-8302.

839 Stefansson, A., Gislason, S.R., 2001. Chemical weathering of basalts, Southwest
840 Iceland: Effect of rock crystallinity and secondary minerals on chemical
841 fluxes to the ocean. *American Journal of Science*, 301(6): 513-556.

842 Stefansson, A., Gislason, S.R., Arnorsson, S., 2001. Dissolution of primary minerals
843 in natural waters - II. Mineral saturation state. *Chemical Geology*, 172(3-
844 4): 251-276.

845 Teng, F.Z., Li, W.Y., Rudnick, R.L., Gardner, L.R., 2010. Contrasting lithium and
846 magnesium isotope fractionation during continental weathering. *Earth*
847 *and Planetary Science Letters*, 300: 63-71.

848 Teng, F.Z. et al., 2004. Lithium isotopic composition and concentration of the
849 upper continental crust. *Geochimica Et Cosmochimica Acta*, 68(20):
850 4167–4178.

851 Thordarson, T., Hoskuldsson, A., 2002. Iceland. *Classic Geology in Europe 3*.
852 Terra Publishing.

853 Tomascak, P.B., Hemming, N.G., Hemming, S.R., 2003. The lithium isotopic
854 composition of waters of the Mono Basin, California. *Geochimica Et*
855 *Cosmochimica Acta*, 67(4): 601-611.

856 Tomascak, P.B., Langmuir, C.H., Le Roux, P.J., Shirey, S.B., 2008. Lithium isotopes
857 in global mid-ocean ridge basalts. *Geochimica Et Cosmochimica Acta*(72):
858 1626-1637.

859 Ullmann, C.V. et al., 2013. Partial diagenetic overprint of Late Jurassic belemnites
860 from New Zealand: Implications for the preservation potential of $\delta^7\text{Li}$
861 values in calcite fossils. *Geochimica Et Cosmochimica Acta*, 120: 80–96.

862 Verney-Carron, A., Vigier, N., Millot, R., Hardarson, B.S., 2015. Lithium isotopes in
863 hydrothermally altered basalts from Hengill (SW Iceland). *Earth and*
864 *Planetary Science Letters*, 411: 62–71.

865 Vigier, N. et al., 2008. Quantifying Li isotope fractionation during smectite
866 formation and implications for the Li cycle. *Geochimica Et Cosmochimica*
867 *Acta*, 72: 780–792.

868 Vigier, N., Gislason, S.R., Burton, K.W., Millot, R., Mokadem, F., 2009. The
869 relationship between riverine lithium isotope composition and silicate
870 weathering rates in Iceland. *Earth and Planetary Science Letters*, 287(3-
871 4): 434–441.

872 Walker, J.C.G., Hays, P.B., Kasting, J.F., 1981. A Negative Feedback Mechanism for
873 the Long-Term Stabilization of Earths Surface-Temperature. *Journal of*
874 *Geophysical Research-Oceans and Atmospheres*, 86(NC10): 9776-9782.

875 Wang, Q.-L. et al., 2015. Behavior of lithium isotopes in the Changjiang River
876 system: Sources effects and response to weathering and erosion.
877 *Geochimica Et Cosmochimica Acta*, 151: 117–132.

878 Wanner, C., Sonnenthal, E.L., Liu, X.-M., 2014. Seawater $\delta^7\text{Li}$: A direct proxy for
879 global CO₂ consumption by continental silicate weathering? *Chemical*
880 *Geology*, 381: 154–167.

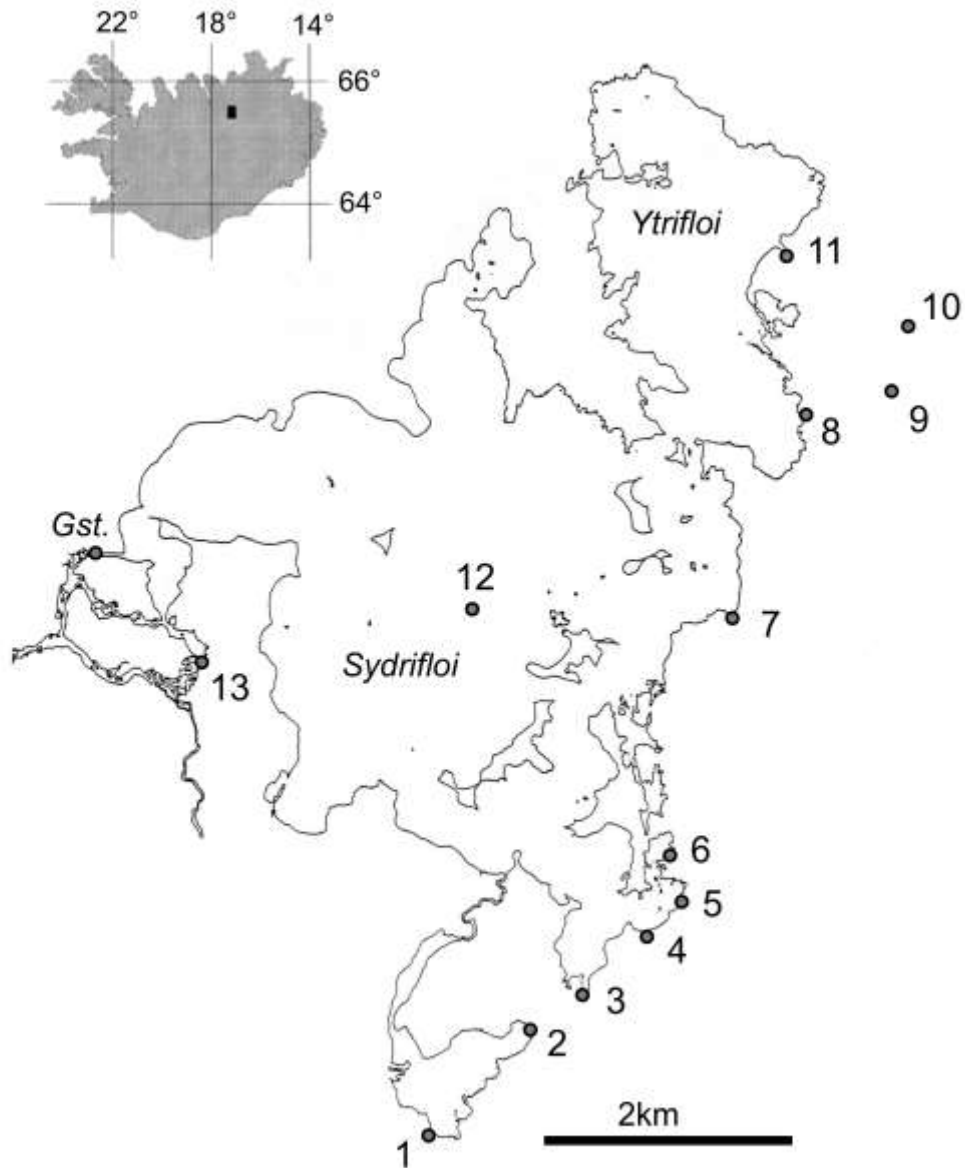
881 Wimpenny, J. et al., 2010a. The behaviour of Li and Mg isotopes during primary
882 phase dissolution and secondary mineral formation in basalt. *Geochimica*
883 *Et Cosmochimica Acta*, 74: 5259-5279.

884 Wimpenny, J. et al., 2010b. Glacial effects on weathering processes: New insights
885 from the elemental and lithium isotopic composition of West Greenland
886 rivers Earth and Planetary Science Letters, 290: 427-437.
887 Witherow, R.A., Berry Lyons, W., Henderson, G.M., 2010. Lithium isotopic
888 composition of the McMurdo Dry Valleys aquatic systems. Chemical
889 Geology, 275: 139–147.
890 Wunder, B., Meixner, A., Romer, R.L., Heinrich, W., 2006. Temperature-dependent
891 isotopic fractionation of lithium between clinopyroxene and high-
892 pressure hydrous fluids. Contributions to Mineralogy and Petrology,
893 151(1): 112-120.
894 Ziegler, K., Chadwick, O.A., Brzezinski, M.A., Kelly, E.F., 2005. Natural variations of
895 delta Si-30 ratios during progressive basalt weathering, Hawaiian Islands.
896 Geochimica Et Cosmochimica Acta, 69(19): 4597-4610.
897

Sample	Sample month	Temperature °C	pH	Conductivity μS/cm	Li nM	Na mM	K mM	Mg mM	Ca mM	Al μM	Si mM	P μM
<i>Input springs</i>												
IC/MY/01.09		3.4	9.27		131	0.53	0.02	0.07	0.11	0.45	0.29	1.4
IC/MY/02.09		7.0	9.40	130	252	0.72	0.03	0.11	0.12	0.53	0.31	1.5
IC/MY/03.09		6.5	9.21	141	279	0.67	0.03	0.15	0.15	0.50	0.30	1.6
IC/MY/04.09		6.2	9.23	129	226	0.64	0.03	0.14	0.14	0.45	0.30	1.7
IC/MY/05.09		5.8	9.60	115	91	0.74	0.02	0.07	0.11	0.67	0.31	1.8
IC/MY/06.09		7.0	9.60	134	101	0.81	0.02	0.08	0.11	0.59	0.34	1.5
IC/MY/07.09		7.5	9.29	156	174	0.90	0.03	0.13	0.16	0.48	0.35	1.7
IC/MY/08.09		16.5	8.68	359	1100	2.02	0.10	0.16	0.30	0.62	1.38	0.9
IC/MY/09.09		37.3	8.29	505	1970	3.32	0.15	0.08	0.35	1.06	2.25	0.5
IC/MY/10.09		44.0	8.10	437	1920	2.64	0.15	0.09	0.28	0.20	2.23	0.5
IC/MY/11.09		24.3	8.29	396	917	1.73	0.10	0.16	0.51	0.32	1.20	0.8
IC/MY/14.09		20.0	3.50	620	10050	2.55	0.27	0.14	0.20			0.6
IC/MY/12.09 - Mid-lake		10.2	9.82	157	227	0.77	0.03	0.11	0.15	0.39	0.15	1.0
IC/MY/13.09 - lake outflow		10.7	10.00	162	236	0.79	0.03	0.12	0.15	0.31	0.13	0.8
<i>Laxa River</i>												
00A013	Mar-00	1.2	8.37		180	1.01	0.04	0.16	0.20	0.33	0.41	
00A023	Apr-00	0.0	9.03		137	0.78	0.03	0.15	0.16	0.03	0.30	
00A031	May-00	6.0	8.52		177	0.75	0.03	0.13	0.15	0.30	0.22	
00A044	Jun-00	12.3	9.63		146	0.88	0.03	0.15	0.18	0.40	0.10	
00A053	Jul-00	15.7	9.93		237	0.95	0.03	0.14	0.18	1.08	0.05	
00A062	Aug-00	15.5	9.78		167	1.04	0.04	0.17	0.20	0.49	0.09	
00A071	Sep-00	8.3	9.35		217	0.94	0.04	0.15	0.18	0.26	0.10	
00A080	Oct-00	1.4	8.73		155	0.95	0.04	0.16	0.18	0.15	0.16	
00A089	Nov-00	0.6	8.32		116	0.97	0.04	0.16	0.19	0.18	0.31	
01A006	Jan-01	0.9	8.34		153	0.97	0.04	0.16	0.19	0.47	0.41	
01A015	Mar-01	0.5	8.43		236	0.88	0.04	0.14	0.14	0.38	0.34	

898

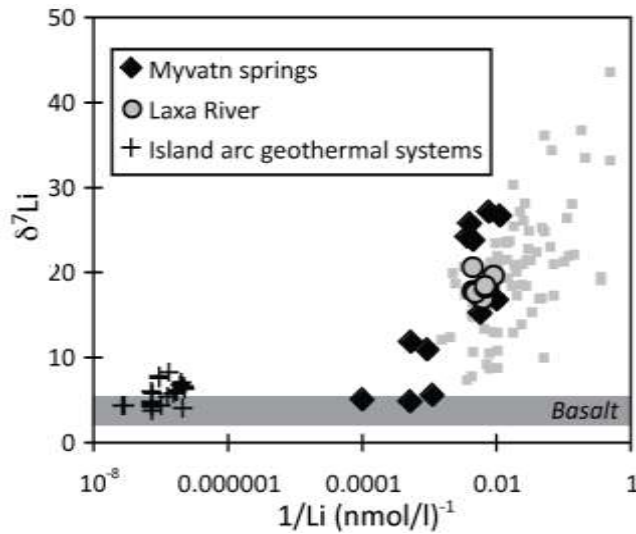
899 Table 1. Physical measurements, trace element concentrations and Li isotopes
900 ratios (‰) from the input springs to Myvatn, and the time series across the
901 outflowing Laxa River. Trace element data aside from Li concentrations are from
902 Opfergelt et al. (2011). Spring pH was measured at their inherent temperature,
903 while river pH was measured at room temperature.



905

906 Figure 1. Sample location map of Lake Myvatn with the two main basins (Ytrifloi
 907 and Sydrifloi): “cold” springs (MY01 to 07), “hot” springs (MY08 to 11), middle
 908 lake water (MY12) and Laxa River outlet (MY13). The monitoring over 2000–
 909 2001 was made at the outlet Geirastadaskurdur (Gst.). From Opfergelt et al.,
 910 2011.

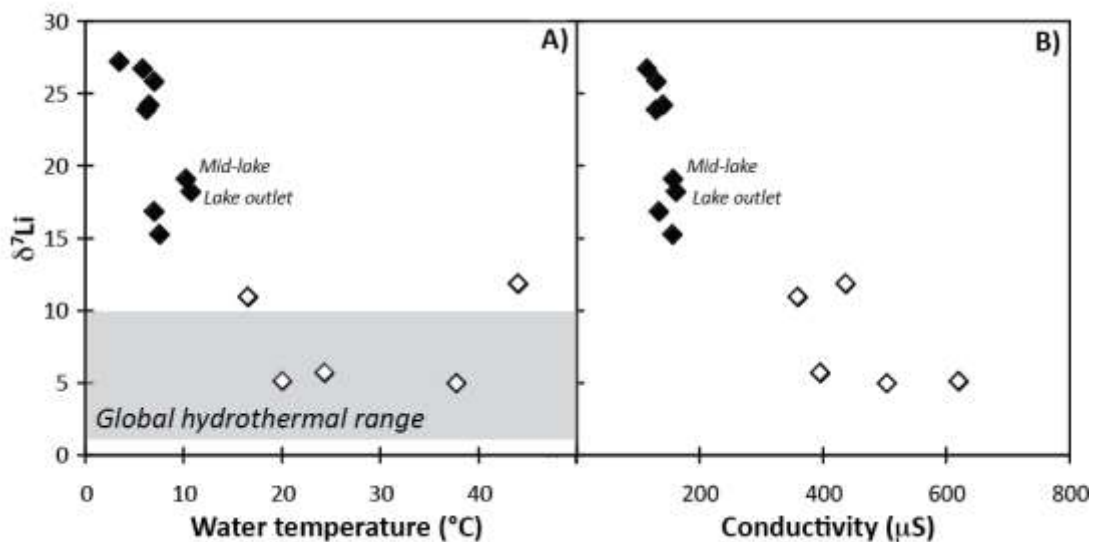
911



912

913 Figure 2. Li isotopes as a function of the reciprocal of the Li concentration. The
914 island arc geothermal systems are from Guadeloupe and Martinique (Millot et al.,
915 2010a). The small grey squares represent other basaltic weathering data from
916 rivers and soil pore waters from Iceland (Pogge von Strandmann et al., 2006;
917 Vigier et al., 2009), the Azores (Pogge von Strandmann et al., 2010), and the
918 Columbia River Basalts (Liu et al., 2015). Typical basaltic $\delta^7\text{Li}$ compositions
919 shown as grey field (Elliott et al., 2006; Tomascak et al., 2008).

920

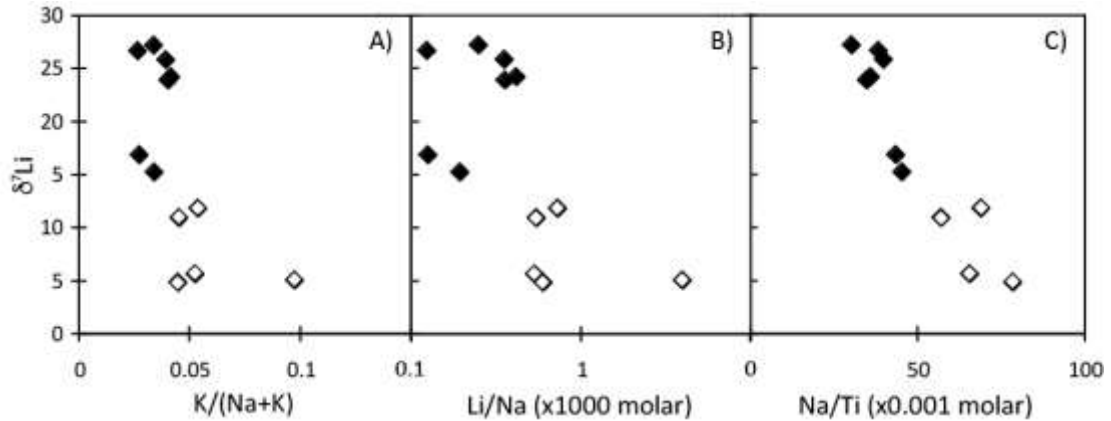


921

922 Figure 3. Li isotope ratios from the source springs to Myvatn, plotted against A)
923 water temperature, and B) conductivity. Open symbols are “hot” springs from
924 geothermal fields, while closed symbols are “cold” groundwaters. The grey field

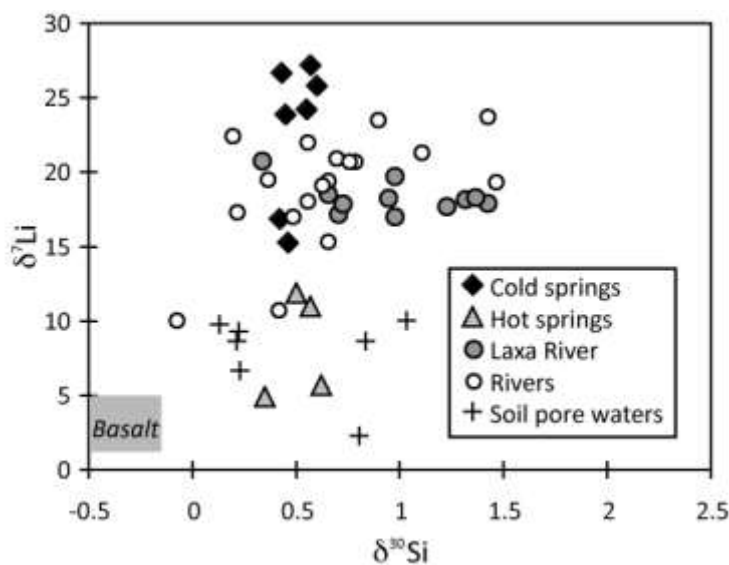
925 denotes the global hydrothermal range of $\delta^7\text{Li}$ values (Chan et al., 1993; Chan et al., 1994; Henchiri et al., 2014; Millot et al., 2010a; Pogge von Strandmann et al., 2010; Pogge von Strandmann et al., 2006).

928



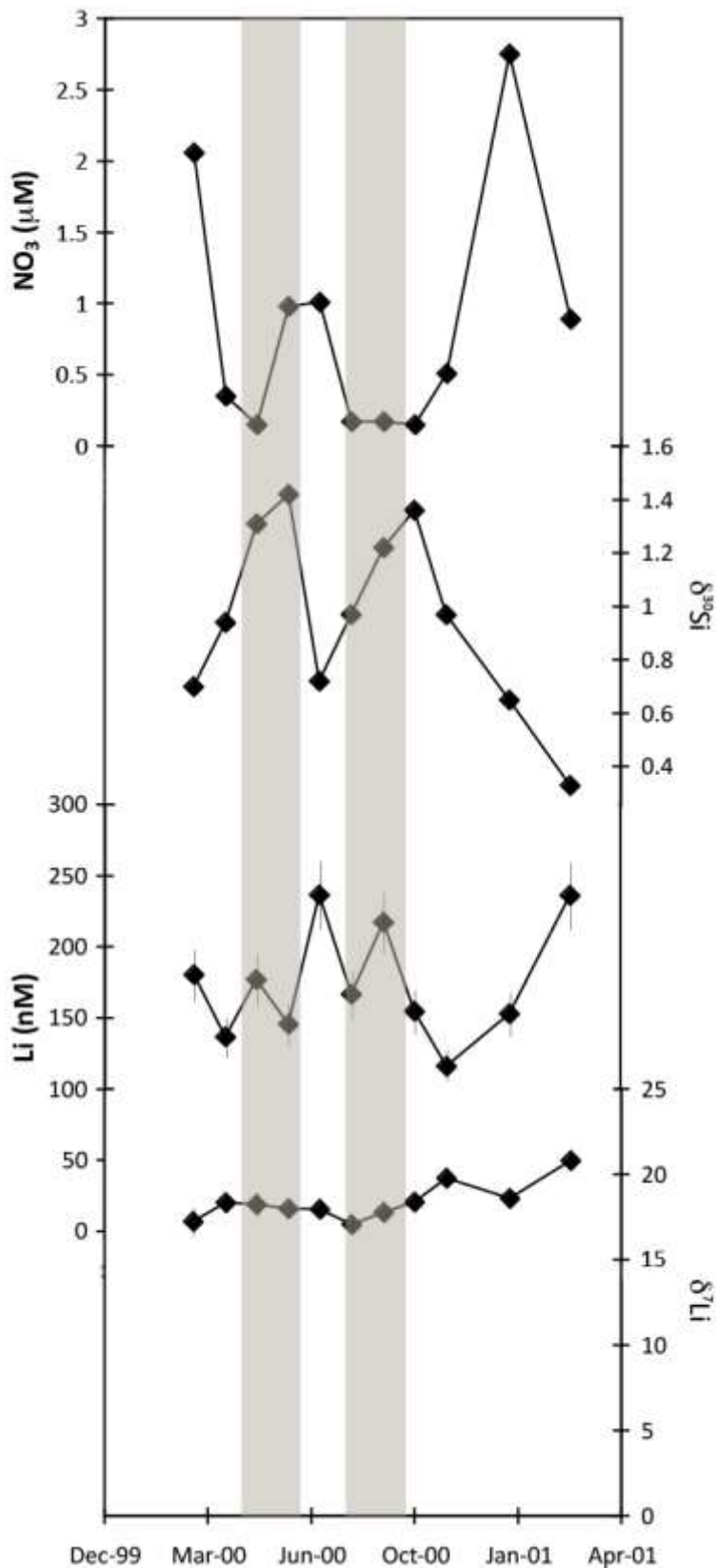
929

930 Figure 4. Li isotopes from Myvatn springs plotted against a series of elemental
 931 tracers of weathering processes. A) $\text{K}/(\text{Na}+\text{K})$, a tracer of weathering regime,
 932 where higher values indicate transport limitation, and lower values weathering
 933 limitation (Edmond et al., 1995; Pogge von Strandmann et al., 2010). B) Li/Na
 934 ratios have been proposed as a tracer of silicate weathering residence time in
 935 monolithologic catchments (Liu et al., 2015). C) Na/Ti ratios show behaviour of a
 936 highly mobile element (Na) relative to an immobile one (Ti). Combined, these
 937 relationships show how powerful Li isotopes are at tracing of silicate weathering
 938 processes. Open symbols are "hot" springs from geothermal fields, while closed
 939 symbols are "cold" groundwaters.



940

941 Figure 5. Li isotopes plotted against Si isotopes for the spring samples and Laxa
942 River (Opfergelt et al., 2011), and Icelandic rivers (Georg et al., 2007; Vigier et al.,
943 2009) and soil pore waters (Pogge von Strandmann et al., 2012). The lack of any
944 correlation suggests that the two systems are controlled by different processes.
945



946

947 Figure 6. Time series from the Laxa River outflow from Lake Myvatn. The NO₃
 948 and δ³⁰Si data (Opfergelt et al., 2011) clearly respond to seasonal productivity
 949 changes (times of spring and autumn diatom blooms highlighted in grey). In

950 contrast, Li concentrations and isotope ratios are unaffected by primary
951 productivity. The small variability in both is likely due to changes in input to the
952 lake. This clearly indicated that Li isotopes are unaffected by primary
953 productivity.

954

955

956